Vapor-Phase Lubrication: Reaction of Phosphate Ester Vapors with Iron and Steel

David W. Johnson* and Samantha Morrow

Department of Chemistry, University of Dayton, 300 College Park, Dayton, Ohio 45469

Nelson H. Forster

Propulsion Directorate, Air Force Research Laboratory, Wright Patterson Air Force Base, Ohio 45433

Costandy S. Saba

University of Dayton Research Institute, 300 College Park, Dayton, Ohio 45469

Received September 27, 2001. Revised Manuscript Received July 12, 2002

Aromatic phosphate esters such as triphenyl phosphate, tricresyl phosphate (TCP), and tri(*tert*-butylphenyl) phosphate, have been degraded in the presence of pure iron or metal alloys such as M-50 or 52100 steel. Among these volatile degradation products are those generated from the addition of an aromatic ring to the phosphate ester. Other products, which have been identified, include substituted biphenyls and diphenyl ethers derived from the decomposition of the above-mentioned addition product. Still other products are fused ring aromatic compounds such as anthracene, which arise from secondary reactions of the initial decomposition reactions. The decomposition reactions leave a nonvolatile phosphate film on the surface of the metal. Characterization of the film with Auger spectroscopy suggests iron phosphate as the product. X-ray photoelectron spectroscopy shows the presence of a bound organic layer at the surface. A mechanism that explains many of the decomposition products and the formation of a bound glassy iron phosphate film is proposed.

Introduction

The requirements for lubrication of gas turbine engines include effective lubrication over a very wide temperature range and the ability to lubricate high-speed rolling element bearings. Vapor-phase lubrication is one method of obtaining effective lubrication over a very broad temperature range. At bearing temperatures below the boiling range of the lubricant, the vapor condenses and functions predominantly as a liquid lubricant. At higher temperatures, vapor lubricants react with metal substrates to augment the liquid film with a solid component chemically reacted on the metal substrate. Of the chemical classes studied for vapor-phase lubricants, triaryl phosphates have proven to be the most viable candidates.[1,2]

Phosphate esters have been used extensively as antiwear additives since before World War II.[3] Despite some recognized problems such as hydrolysis[4] and neurotoxicity,[5] these compounds have become commercially important in many products due to their stability, high ignition temperature, low heats of combustion, and boundary lubrication characteristics.[6] In more recent times, beginning with the work of Klaus, these compounds have found added uses in vapor-phase lubrication.[7]

Triaryl phosphates have been shown to form a lubricious film on several different materials. Makki and Graham speculated that the presence of a reactive oxide layer on the surface is required to form a tenacious and lubricious film.[8] If the bearing material does not contain the proper reactive oxide layer, the film, which forms at the surface, is not durable.[9] Ceramics[10] and other high-temperature alloys,[11] for example, must be coated with an iron oxide film by deposition of ferric acetylacetonate or electrodeposition of iron oxide for vapor-phase lubrication to be effective.

The test sample, which formed a solid lubricious film, is known to contain a polymeric film on the surface with a molecular weight in the range of 6000−60000 g/mol.[12] Previous work indicates, using infrared spectroscopy, that the film contains a mixture of phosphate and probably polyphosphate ions.[13] Surface analyses of bearings indicate the presence of carbon, phosphorus, oxygen, and iron at varying levels in the surface film.[14]

* To whom correspondence should be addressed.

(1) Forster, N. H.; Trivedi, H. K. *Tribol. Trans.* **1997**, *40*, 421.
(2) Forster, N. H.; Trivedi, H. K. *Tribol. Trans.* **1997**, *40*, 493.
(3) Beek, O.; Given, J. W.; Williams, E. C. *Proc. R. Soc. (London), Ser. A* **1940**, *968*, 102.
(4) Bieber, H. E.; Klaus, E. E.; Tewksbury, E. J. *ASLE Trans.* **1968**, *11*, 155.
(5) Wyman, J. F.; Porvaznik, M.; Serve, P.; Hobson, D.; Uddin, D. E. *J. Fire. Sci.* **1987**, *5*, 162.
(6) Marino, M. P. *Chem. Ind.* **1993**, *48*, 67.
(7) Graham, E. E.; Klaus, E. E. *ASLE Trans.* **1986**, *29*, 229.
(8) Makki, J.; Graham, E. E. *Lubr. Eng.* **1991**, *47*, 199.
(9) Hanyaloglu, B.; Graham, E. E. *Lubr. Eng.* **1993**, *49*, 227.
(10) Hanyaloglu, B.; Graham, E. E. *Lubr. Eng.* **1994**, *50*, 814.
(11) Hanyaloglu, B.; Fedor, D. C.; Graham, E. E. *Lubr. Eng.* **1995**, *51*, 252.
(12) Hanyaloglu, B. F.; Graham, E. E.; Oreskovic, T.; Hajj, C. G. *Lubr. Eng.* **1995**, *51*, 503.

10.1021/cm010921o CCC: $22.00
Published on Web 08/17/2002

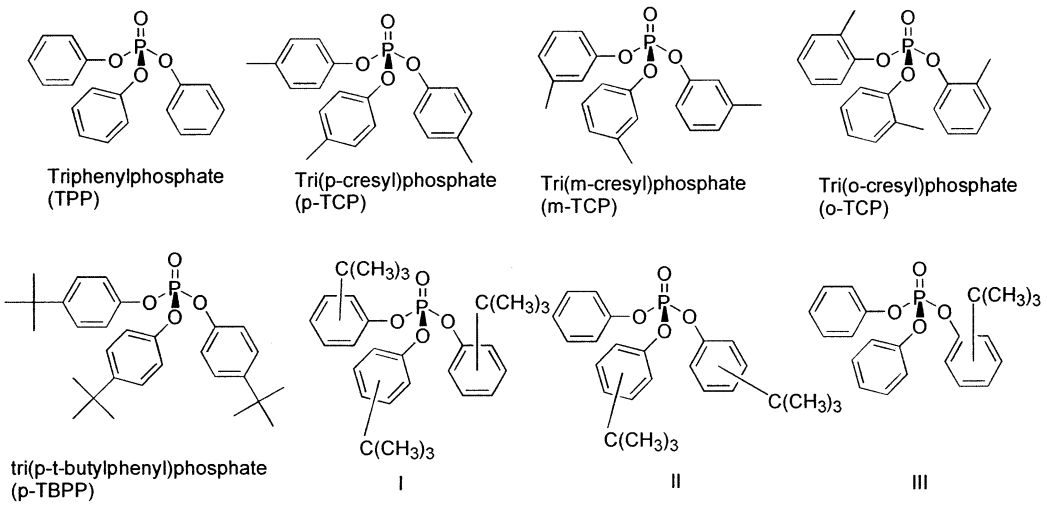

Figure 1. Structures for some of the phosphate esters used in this study.

As part of the lubrication mechanism, the diffusion of iron into the phosphate layer was hypothesized to be important.[15] In other studies, Klaus et al. concluded that there were other forms of iron (iron carbide and iron phosphide) in some layers that were removed as sticky tape samples.[16] In liquid lubricants, it has been suggested that deposition of an iron phosphate-containing layer onto a bearing surface reduced friction substantially, although iron phosphate itself is not a good lubricant.[17]

In this paper, we describe experiments that have allowed us to identify many of the initial degradation products from the interaction of triaryl phosphates with iron foil and metal alloy samples in the temperature range of 400−475 °C. We also present surface analysis data identifying the chemical composition of the surface and subsurface layers of the metal coupon. Using this information, we propose a mechanism for the formation of a chemically bound lubricious, polymeric film on the metal surface. This mechanism leads to a greater understanding of the vapor-phase lubrication process and the mode of action of phosphate ester-based antiwear additives.

Experimental Methods

A. Materials. Iron foil samples (99.999%), coupons made from 52100, M-50, and 440C steel, and triphenyl phosphate were purchased commercially. The structures of the model compounds used in this study are shown in Figure 1. Model compounds, tri(*p*-cresyl) phosphate (*p*-TCP) and tri(*m*-cresyl) phosphate (*m*-TCP), were purchased from Eastman Kodak and tri(*p*-*tert*-butylphenyl) phosphate (*p*-TBPP) was synthesized by methods that have been previously reported.[18] The resulting compounds were analyzed by gas chromatography/mass spectrometry and shown to be >99% pure. A commercial phosphate ester lubricant (com. *t*-BPP) consisting of a mixture of various isomers (primarily meta and para) of compounds I, II, III, and TPP (Figure 1) was purchased from FMC, Inc.

B. Sample Preparation. Iron foil, 52100, and M-50 steel test coupons (approximately 1-cm square) were inserted into a new 16 × 150 mm glass test tube. The tube was evacuated and flame-dried. After cooling, a small (≈25 mg or 25 μL) sample lubricant was added to the tube and the tube was evacuated to a pressure of <0.5 Torr. The sample tubes were flame-sealed, allowed to cool, then placed in a furnace, and heated for the time and temperatures specified. The tubes were removed from the furnace and cooled to room temperature. Each tube was reweighed. Only those tubes that showed insignificant change in mass (<0.0005 g) were kept for further analysis. The tubes were broken open, the metal coupons were removed, and 5 mL of toluene was added to dissolve the residue. These solutions were analyzed by gas chromatography/mass spectrometry to determine the extent of lubricant degradation and identify the degradation products. The metal coupons were then reweighed to determine the mass of the film. Iron foils and metal alloy samples, along with each of the model compounds, were heated at temperatures of 400, 425, 450, and 475 °C for reaction times of 15 min, 30 min, 1 h, 2 h, 4 h, 8 h, and 24 h. A blank was prepared for each of the phosphate esters and run for 24 h at each of the temperatures used in this study.

C. Gas Chromatography/Mass Spectrometry. Gas chromatography/mass spectrometric analysis was conducted on each of the stressed and unstressed lubricant samples. The injector was operated in a splitless mode at a temperature of 350 °C. The column (HT-5, 100-μm film thickness, 25-m length) was heated from an initial temperature of 130 °C for 2 min, increasing at 10 °C/min to 325 °C and holding at 325 °C for 15 min. Mass spectral data were collected over the mass range of 50−700 amu with a peak threshold of 100 counts. The mass spectrometer was calibrated daily using perfluorotributylamine throughout this work. Compounds were identified by comparison of their mass spectra with mass spectra contained in the NIST Library of Mass Spectra[19] with a minimum match quality of 90 used for identification. The mass spectra of compounds not contained in the library were interpreted using techniques described by McLafferty.[20] All compounds identified in this way showed strong molecular ion peaks, as is common for aromatic compounds in electron impact mass spectrometry and fragment ions that are appropriate for the compound identification.[21]

(13) Morales, W.; Hanyaloglu, B.; Graham, E. E. *Infrared Analysis of Vapor Deposited Tricresylphosphate*; NASA Technical Memorandum 106423; NASA Lewis Research Center: Cleveland, OH, Jan 1994.
(14) Forster, N. H. *Tribol. Trans.* **1999**, *42*, 1.
(15) Forster, N. H. *Tribol. Trans.* **1999**, *42*, 10.
(16) Klaus, E. E.; Philips, J.; Lin, S. C.; Duda, J. L. *Tribol. Trans.* **1990**, *33*, 25.
(17) Wang, S. S.; Tung, S. C. *Tribol. Trans.* **1991**, *34*, 45.
(18) Krishnakumar, V. K.; Sharma, M. M. *Synthesis* **1983**, *7*, 558.
(19) Standard Reference Data Program, National Institute of Standards and Technology, Gaithersburg, MD, Standard Reference Database 1A.
(20) McLafferty, F. W. *Interpretation of Mass Spectra*; University Science Books: Mill Valley, CA, 1980; pp 119−167.
(21) Litzow, M. R.; Spalding, T. R. *Mass Spectrometry of Inorganic and Organometallic Compounds*; Elsevier Scientific: New York, 1973; pp 321−439.

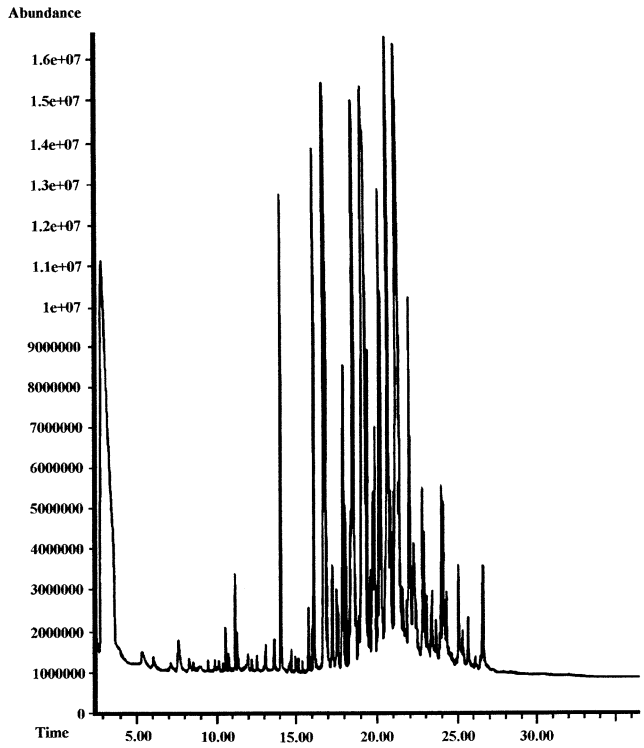

Figure 2. Total ion chromatogram for the thermal degradation of commercial *t*-BPP in the presence of 52100 alloy at 400 °C for 3 h.

D. Surface Analysis. Iron foil samples were analyzed by Auger electron spectroscopy (AES) and X-ray photoelectron spectroscopy (XPS). Auger depth profiles were measured using a sputter rate of 80 Å/min and are presented as at. % on each surface. XPS data were collected at an incident angle of 10°, which corresponds to a penetration depth of ≈30 Å. A few samples were also run at an angle of 60°, which corresponds to a penetration of 15 Å. There was no discernible difference between the 10° and 60° spectra.

E. Fourier Transform Infrared Spectroscopy. Fourier transform infrared spectra of deposits on the metal coupons were collected using a Fourier transform infrared spectrometer equipped with a microscope in reflectance mode. Spectra were collected at several positions on the metal surface to obtain representative results. Infrared spectra of the residual mixtures were measured in transmission mode between KBr disks.

Results

Preliminary experiments were conducted using commercial phosphate esters that contained between 4 and 10 compounds, initially. After reaction, the mixture was extremely complex, as is shown in Figure 2. This observation led us to investigate the reactions of a small number of the components in the mixture. Triphenyl phosphate, tri(*p*-cresyl) phosphate, tri(*m*-cresyl) phosphate, and tri(*tert*-butylphenyl) phosphate were chosen as model compounds. These compounds are components of the commercial phosphate ester lubricants and are expected to mimic the chemistry of the mixture.

All of the metal foil samples were visibly coated after even the shortest of the reaction times. For the shorter times, the coating appeared as a slight discoloration of the surface. For the longer reaction times a visible dark coating was deposited on the metal. Each metal coupon also showed a measurable increase in mass ranging between 0.5 and 2.5 mg. The mass increases were largest for the foils heated for longer times at higher temperatures.

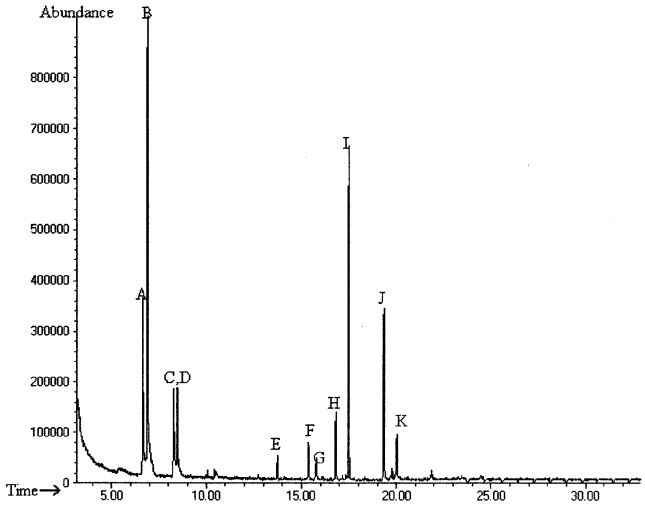

Figure 3. Total ion chromatogram and product identification for the thermal degradation of triphenyl phosphate in the presence of 52100 alloy at 450 °C for 2 h.

A. Volatile Degradation Products. The toluene solutions obtained from each of the sealed tube tests showed evidence of reaction through the introduction of color to the solution. The solutions from the lower temperature tests were light amber in color while the solutions from the higher temperature tests were brown. These samples were all analyzed by gas chromatography/mass spectrometry. The total ion chromatogram for each was recorded and the areas presented below are from the integration of the total ion chromatogram. Care must be exercised in the interpretation of these areas due to the differences in the ionization efficiency of the various compounds and the possibility that detector saturation may have occurred for some of the components with high concentrations.[22]

1. Reaction of Triphenyl Phosphate. Triphenyl phosphate is the most stable molecule among the model compounds. This stability was evident not only in its clean degradation pattern but also in the observation that significant degradation did not occur at 400 °C for up to 4-h exposure times. The total ion chromatogram for a sample of triphenyl phosphate degraded at 450 °C for 2 h is shown in Figure 3. The degradation products along with the area percentages are listed in Table 1. Structures for selected degradation products are shown in Figure 4. One likely product, which is not shown in the chromatogram, is phenol, which co-elutes with the solvent toluene. A second sample where the residue was dissolved in acetone shows the presence of phenol in the mixture.

The products of the reactions include some higher molecular weight compounds, which are derived from the addition of an aromatic ring to triphenyl phosphate (J,K in Figure 3). These two compounds are isomers, differing in the placement of the added aromatic ring most likely at the meta and para position. Many of the other compounds formed appear to be decomposition, fragmentation, and recombination products including biphenyl (A), diphenyl ether (B), and *o*-hydroxybiphenyl

(22) Message, G. M. *Practical Aspects of Gas Chromatography/Mass Spectrometry*; John Wiley and Sons: New York, 1984; pp 313−316.

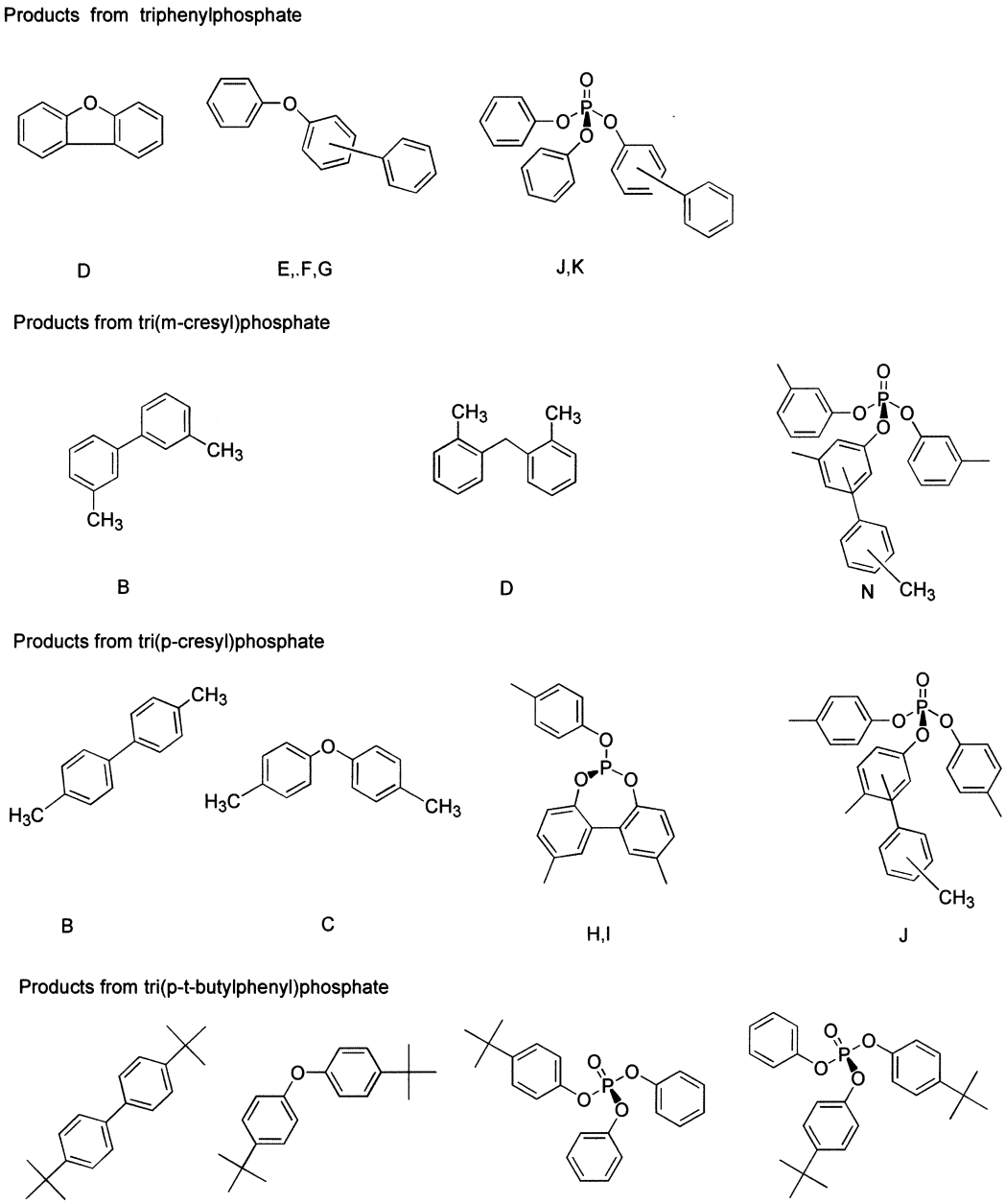

Figure 4. Structures of some of the major products formed in the reaction of phosphate esters with iron.

Table 1. Gas Chromatography/Mass Spectrometry Data for the Degradation of Triphenyl Phosphate with 52100 Steel

			area percentage					
	R.T. (min)	identification	2 h/ 400 °C	24 h/ 400 °C	2 h/ 425 °C	24 h/ 425 °C	2 h/ 450 °C	24 h/ 450 °C
A	6.64	biphenyl	ND	13.71	8.45	24.56	22.34	38.45
B	6.88	biphenyl ether	ND	32.42	11.23	14.98	16.55	15.45
C	8.28	*o*-hydroxybiphenyl	ND	7.04	2.92	4.09	5.05	5.95
D	8.47	dibenzofuran	ND	7.14	3.87	6.47	7.02	2.03
E, F	13.75−15.37	phenyl diphenyl ether derivatives	ND	4.06	5.12	3.78	5.04	3.23
G	15.79	3-phenyl diphenyl ether	ND	1.86	3.02	4.56	3.69	1.23
H	16.8	MW = 277 (unidentified)	ND	3.95	4.56	7.94	6.09	2.09
I	17.48	TPP	99.04	16.66	44.56	8.32	16.34	4.04
J, K	19.35−20.02	phenyl TPP	ND	1.34	3.33	18.23	11.23	22.1

(C), which can be formed through cleavage of either the O−P or the O−C bond in products J and K.

2. Reaction of Tricresyl Phosphate: Typical total ion chromatograms for the decomposition of tri(*p*-cresyl) phosphate (*p*-TCP) and tri(*m*-cresyl) phosphate (*m*-TCP) at 400 °C for 24 h in the presence of iron are shown in Figures 5 and 6, respectively. Decomposition of the phosphate esters in the absence of iron produces mainly phenol, consistent with previous observations.[23] The presence of the iron significantly alters the decomposition pathway, yielding a more complex mixture of

(23) Paciorek, K. J. L.; Kratzer, R. H.; Kaufman, J.; Nakahara, J. H.; Christos, T.; Harstein, A. M. *Am. Ind. Hyg. Assoc. J.* **1978**, *39*, 633.

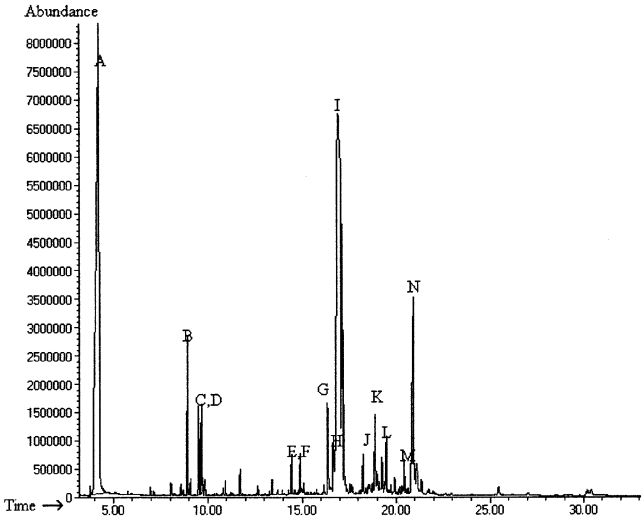

Figure 5. Total ion chromatogram and product identification for the thermal degradation of tri(*m*-cresyl) phosphate in the presence of 52100 alloy at 400 °C for 24 h.

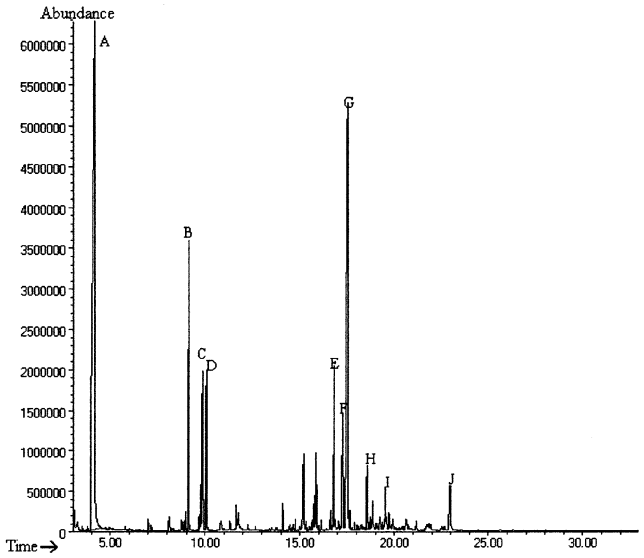

Figure 6. Total ion chromatogram and product identification for the thermal degradation of tri(*p*-cresyl) phosphate in the presence of 52100 steel at 400 °C for 24 h.

products. The results presented in Tables 2 and 3 are primarily for the identification of the products and approximate amounts.

The meta and para isomers of tricresyl phosphate have similar degradation products. The primary products are cresol and several isomers of tolyl-tricresyl phosphate (tolyl-TCP), which differ in the placement of the methyl group on the aromatic ring. The two compounds do, however, show significant difference in the minor degradation products. Structures of selected products are shown in Figure 4.

The degradation products of *m*-TCP are shown in Figures 4 and 5 and Table 2. In addition to *m*-cresol and tolyl-TCP, significant quantities of other aromatic compounds such as dimethylbiphenyl, dimethyl diphenyl ether, and methylene bis(methylbenzene) are formed. The products are viewed as the decomposition products of tolyl-TCP. Another group of products that have been identified as minor products from *m*-TCP are the fused-ring aromatic compounds, which include 9-H fluorene, anthracene, and phenanthrene. A final product has been identified as tricresyl phosphite formed by the reduction of tricresyl phosphate.

The decomposition pattern for *p*-TCP is much simpler (Figure 6) due to the increased stability of the para isomer. In addition to cresol and tolyl-TCP, seven other products have been identified. Three of the products are isomers of products observed from the reaction of *m*-TCP, including dimethylbiphenyl, dimethyl diphenyl ether, and methylene bis(methylbenzene). The fourth and fifth products are identified as linear three-ringed aromatic compounds connected either through methyl groups or directly through the aromatic rings. The sixth product is TCP after the abstraction of one of the methyl groups. The final product is tricresyl phosphite. In some samples an additional product is observed with a molecular weight of 548 amu corresponding to the addition of two aromatic rings to TCP. This product is important because it provides one of the pathways for the formation of the three-ringed aromatic compounds described earlier.

Several other minor products are observed in the GC-MS analysis of *m*-TCP and *p*-TCP samples, particularly those at higher temperatures. These products are due to the transfer of methyl groups among the TCP molecules. In this mixture, the methyl groups are scrambled, resulting in the formation of different isomers of TCP. Of particular concern are products where the methyl group is in the ortho position due to the neurotoxicity of tri(*o*-cresyl) phosphate. Several of the products were identified as having methyl groups in the ortho position. Apparently, degradation can occur, forming ortho isomers from compounds engineered to minimize the formation of the neurotoxic ortho isomers.

3. Degradation Studies of Tri(p-tert-butylphenyl) Phosphate (p-TBPP). The degradation of *p*-TBPP was studied in the presence of iron and M-50 steel. The degradation pattern is similar for both metal samples, although the reactivity of the iron foil is substantially greater than the M-50 alloy. The total ion chromatogram and the product distribution for samples of *p*-TBPP are shown in Figure 7 and Table 4, respectively. Some of the structures of degradation products are shown in Figure 4.

The presence of the iron foil greatly increases both the diversity of products and the reactivity of the phosphate ester relative to a blank where the metal is absent. The primary degradation products were similar to those observed for *p*-TCP, including *tert*-butyl phenol and an addition product where a *tert*-butyl phenyl group is added to a molecule of *p*-TBPP. Other products formed at higher temperatures and longer reaction times include products where the *tert*-butyl groups are lost and other products where an additional *tert*-butyl group has been added.

Lower molecular weight products such as di(*tert*-butyl)biphenyl and di(*tert*-butyl phenyl) ether are observed in the mixture as well. Some samples are observed to contain fused-ring aromatic compounds in addition to the compounds described above. Another class of products observed is reduction products of the phosphate ester, which have a molecular weight 2 less than the parent phosphate ester molecule. These products are likely due to the loss of hydrogen, forming a

Table 2. Gas Chromatography/Mass Spectrometry Data for the Degradation of Tri(*m*-cresyl) Phosphate with 52100 Steel

chromatography data			area percentages								
			400 °C			425 °C			450 °C		
peak	R.T.	identification	2 h	4 h	24 h	2 h	4 h	24 h	2 h	4 h	24 h
A	4.23	*m*-cresol	8.31	13.85	31.35	13.63	17.99	22.44	11.14	12.74	33.49
B	8.94	dimethylbiphenyl	<0.1	0.36	2.41	<0.1	0.29	1.19	<0.1	<0.1	1.52
C	9.52	dimethyl diphenyl ether	0.20	0.38	1.31	<0.1	0.20	0.57	<0.1	<0.1	1.23
D	9.68	methylene bis(methylbenzene)	0.41	0.75	2.12	<0.1	0.32	1.31	<0.1	<0.1	1.41
E	14.44	trimethylterphenyl	<0.1	<0.1	0.47	<0.1	<0.1	0.42	<0.1	<0.1	0.30
F	14.89	dimethylbiphenyl methylphenyl ether	<0.1	<0.1	0.54	<0.1	<0.1	0.57	<0.1	<0.1	0.59
G	16.36	dicresylphenyl phosphate	1.07	1.04	1.87	1.24	1.57	2.42	1.05	0.97	2.52
H	16.65	TCP	1.26	1.08	1.53	<0.1	0.43	0.46	0.42	1.02	N.D.
I	16.92	*m*-TCP	76.60	62.36	37.70	74.23	63.53	46.02	83.25	79.94	42.56
J	17.22	tricresyl phosphite	2.18	<0.1	1.69	0.67	2.63	2.09	0.50	0.81	4.68
K	18.26	TCP−water	<0.1	1.04	<0.1	<0.1	0.56	0.40	<0.1	<0.1	0.35
M	19.50	TCP−water	<0.1	1.45	<0.1	<0.1	1.58	0.53	<0.1	<0.1	0.34
N	20.93	tolyl-TCP	6.20	8.94	9.05	1.38	7.58	11.45	3.05	5.52	12.32

Table 3. Gas Chromatography/Mass Spectrometry Data for the Degradation of Tri(*p*-cresyl) Phosphate with 52100 Steel

			area percentages								
	R.T. (min)	compound	2 h/ 400 °C	8 h/ 400 °C	24 h/ 400 °C	2 h/ 425 °C	8 h/ 425 °C	24 h/ 425 °C	2 h/ 450 °C	8 h/ 450 °C	24 h/ 450 °C
A	4.184	*p*-cresol	7.41	14.64	38.99	3.93	8.82	29.93	5.45	8.34	19.87
B	9.129	dimethylbiphenyl	N.D.	1.17	7.81	N.D.	0.29	3.85	N.D.	N.D.	1.49
C	9.853	dimethyl diphenyl ether	N.D.	2.35	3.53	N.D.	0.36	1.53	N.D.	0.35	1.00
D	10.083	trimethylbiphenyl	N.D.	0.25	3.98	N.D.	N.D.	2.46	N.D.	N.D.	1.54
E	16.824	TCP−methyl	0.40	2.08	3.89	0.51	1.74	5.28	N.D.	1.01	5.15
F	17.269	tricresyl phosphite	N.D.	2.08	4.29	N.D.	N.D.	3.33	N.D.	N.D.	0.32
G	17.588	tri(*p*-cresyl) phosphate	87.31	69.42	18.40	93.91	74.67	37.45	92.33	78.00	56.19
H	18.564	TCP−water	N.D.	0.67	1.12	0.39	1.26	0.73	0.88	N.D.	0.25
I	19.543	TCP−water	N.D.	0.84	1.84	N.D.	0.77	1.04	N.D.	0.39	0.43
J	23.033	tolyltricresyl phosphate	3.10	5.77	2.05	1.26	8.31	3.65	1.34	11.48	10.39

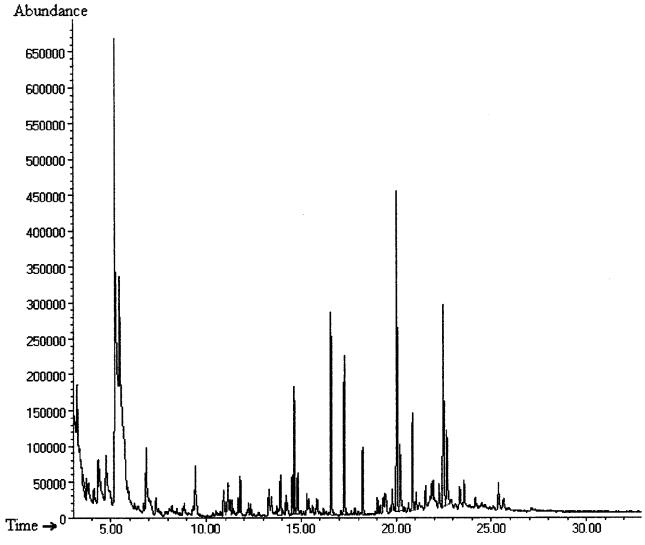

Figure 7. Total ion chromatogram and product identification for the thermal degradation of tri-*tert*-butyl phenyl phosphate in the presence of 52100 alloy at 400 °C for 24 h.

carbon−carbon bond between two rings of the phosphate ester. The formation of a carbon−carbon bond between the two ortho carbon atoms would result in the formation of a seven-membered ring.

At temperatures of 450 °C and above, the majority of the volatile degradation products do not contain phosphorus, suggesting that the formation of a film containing phosphate on the metal surface has consumed the phosphate-containing portion of the molecule. These observations suggest that *p*-TBPP is the most reactive of the phosphate esters studied. This may be due in part to the greater stability of the *tert*-butyl radical compared to that of the methyl radical,[24] which allows for more rapid formation of the phosphate film on the metal surface.

4. Vapor-Phase Degradation of a Commercial tert-Butylphenyl Phosphate Ester (t-BPP). Degradation of *t*-BPP in the presence of an iron coupon proceeds at a much lower temperature than that in the absence of the metal. Figure 1 shows the total ion chromatogram for a sample of *t*-BPP, degraded for 3 h at 400 °C. The majority of the products shown in this chromatogram are the various compounds and isomers in *t*-BPP and compounds that arise from the transfer of a *tert*-butylphenyl group to a molecule of *t*-BPP. Other compounds that have been identified include *tert*-butylphenol, di(*tert*-butylphenyl) ether, and di-*tert*-butylbiphenyl. These products are very similar to the products arising from the other phosphate esters that we have studied. Under similar conditions in the absence of the metal coupon, only a small amount of *tert*-butylphenol is observed.

B. Analysis of the Metal Surface. *1. X-ray Photoelectron Spectroscopy.* X-ray photoelectron spectra were collected for all of the iron foil samples exposed to tri(*p*-*tert*-butylphenyl) phosphate (*p*-TBPP) and a commercial phosphate ester containing *tert*-butylphenyl phosphate (*t*-BPP). The surface composition of the foils is shown in Table 5. Iron foils exposed to the *p*-TBPP show a surface layer, which contains more than 40 at. % carbon and 5−25 at. % of each iron, phosphorus, and oxygen. Significant differences in the outermost layer are not apparent. The film does contain large amounts of C−H bonded carbon and a smaller amount of C−O

(24) March, J. *Advanced Organic Chemistry: Reactions, Mechanisms and Structure*; McGraw-Hill: New York, 1968; pp 126, 155.

Table 4. Gas Chromatography/Mass Spectrometry Data for the Degradation of Tri(*p-tert*-butylphenyl) Phosphate with 52100 Steel

		area percentages							
	compound	2 h/ 400 °C	4 h/ 400 °C	8 h/ 400 °C	24 h/ 400 °C	2 h/ 425 °C	4 h/ 425 °C	8 h/ 425 °C	24 h/ 425 °C
A	*tert*-butylbenzene	0.202	0.348	2.522	3.004	0.607	1.489	1.937	3.961
B	*tert*-butyltoluene	0.063	0.212	0.511	1.816	2.49	1.248	1.494	3.515
C	*tert*-butylphenol	7.568	6.767	16.237	13.628	40.077	11.613	20.897	10.052
D	di(*tert*-butylphenyl)ether	0.098	0.321	0.434	0.308	N.D.	0.169	0.423	0.486
E	di(*tert*-butyl)biphenyl	N.D.	N.D.	0.118	0.524	N.D.	N.D.	0.884	0.296
F	*tert*-butylphenyldiphenyl phosphate	1.415	50236	7.436	13.019	14.808	7.898	10.664	N.D.
G	*tert*-butylphenyldiphenyl phosphate	N.D.	N.D.	1.19	2.94	1.692	1.062	2.015	N.D.
H	di(*tert*-butylphenyl)phenyl phosphate	0.656	3.198	2.912	1.421	1.089	5.781	4.856	N.D.
I	di(*tert*-butylphenyl)phenyl phosphate	N.D.	N.D.	0.649	3.77	N.D.	1.532	1.56	N.D.
J	di(*tert*-butylphenyl)phenyl phosphate	N.D.	N.D.	0.491	1.111	N.D.	1.231	1.719	N.D.
K	tri(*tert*-butylphenyl) phosphate	N.D.	0.748	2.686	1.341	N.D.	1.943	1.587	N.D.
L	tri(*tert*-butylphenyl) phosphate	0.563	5.74	3.907	3.165	1.158	11.249	7.399	N.D.
M	tri(*p-tert*-butylphenyl) phosphate	87.192	72.479	43.385	8.211	13.161	32.68	23.889	N.D.
N	TBPP−hydrogen	N.D.	N.D.	0.739	1.966	N.D.	0.997	6.517	N.D.
O	TBPP−hydrogen	1.759	2.728	1.645	0.313	N.D.	1.184	N.D.	N.D.
P	TBPP−hydrogen	N.D.	N.D.	1.461	N.D.	N.D.	N.D.	N.D.	N.D.

Table 5. X-ray Photoelectron Spectroscopic Data for the Surface Composition of Iron Foil Samples Exposed to Phosphate Esters at High Temperatures

					O			
	time	temp	C		O−H,	O−P,	P	
lubricant	(min)	(°C)	C−O	C−H	C−O	O−Fe	Fe	P−O
com-*t*-BPP	15	400	5.9	36.7	13.6	24.2	11.4	8.2
p-TBPP	15	400	5.8	57.1	9.3	15.7	4.9	4.9
com-*t*-BPP	30	400	7.8	37.7	11.8	24.9	8.2	8.4
p-TBPP	30	400	10.9	54.9	9.7	14.8	3.7	5.4
com-*t*-BPP	60	400	8.2	37.4	13.4	23.2	8.6	8.2
p-TBPP	60	400	12.8	59.2	7.9	11.1	3.1	4.4
com-*t*-BPP	120	400	8.7	32.7	15.6	24.5	8.8	9.7
p-TBPP	120	400	8.6	67.9	9.2	6.4	1.7	2.8
com-*t*-BPP	15	425	7.3	36.3	8.6	26.5	10.9	7.6
p-TBPP	15	425	7.7	52.2	10.0	18.8	4.7	5.8
com-*t*-BPP	30	425	8.7	36.7	9.8	24.1	10.5	7.2
p-TBPP	30	425	8.9	36.3	13.8	21.0	11.2	8.5
com-*t*-BPP	60	425	7.7	65.0	9.5	6.0	1.1	3.4
p-TBPP	60	425	9.8	57.4	8.1	15.0	4.7	4.7
com-*t*-BPP	120	425	8.5	41.8	11.4	15.8	4.7	6.6
p-TBPP	120	425	13.2	41.6	15.0	19.7	5.4	7.7

bonded carbon. The film contains large amounts of oxygen in a C−O bonded mode and also a large amount in the O−P or O−Fe bonded mode. The composition of the surface film is consistent with the formation of an iron organophosphate layer at the surface of the foil. The presence of significant amounts of iron demonstrates that the layer is not simply a layer of solvent or unreacted phosphate ester, which is adsorbed on the metal surface. In addition, the presence of significant quantities of C−O and C−H rules out the possibility of the formation of a layer of amorphous carbon at least in the surface deposit.

2. Auger Electron Spectroscopy. Auger depth profiling was used to examine the thickness of the film and to study any possible layering within the film. The film thicknesses as determined by Auger are shown in Table 6. All of the films have been found to be more than 200-Å thick with more than one layer apparent in the film. The chemical composition of the deposited film and the layered structure are similar to films deposited during actual bearing tests.[25] The surface film on each of the metal coupons has three distinct layers as is shown in Figure 8.

(25) Forster, N. H. High-Temperature Lubrication of Rolling Contacts with Lubricants Delivered from the Vapor Phase and as Oil Mists. WL-TR-97−2003, 1997; pp 46−49.

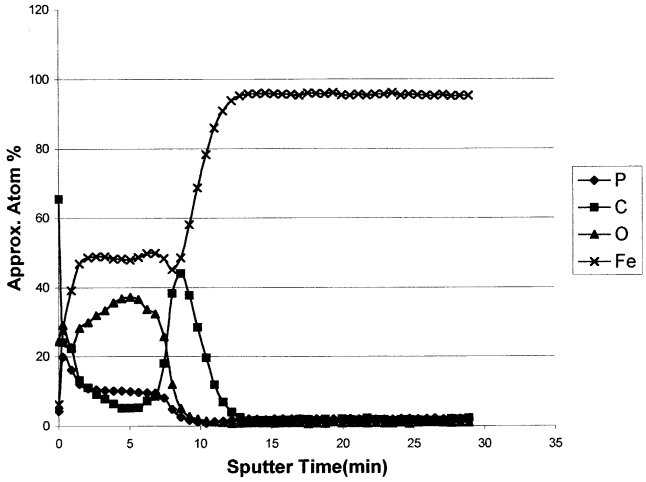

Figure 8. Auger depth profile for the reaction film formed by the reaction of commercial *t*-BPP with iron foil for 2 h at 425 °C.

Table 6. Film Thickness Results for Iron Foils Exposed to High Temperatures in the Presence of *p*-TBPP and Commercial *t*-BPP

lubricant	time (min)	temp (°C)	film thickness (Å)
com-*t*-BPP	15	400	330
p-TBPP	15	400	490
com-*t*-BPP	30	400	830
p-TBPP	30	400	420
com-*t*-BPP	60	400	580
p-TBPP	60	400	560
com-*t*-BPP	120	400	990
p-TBPP	120	400	500
com-*t*-BPP	15	425	680
p-TBPP	15	425	1300
com-*t*-BPP	30	425	410
p-TBPP	30	425	690
com-*t*-BPP	60	425	960
p-TBPP	60	425	1600
com-*t*-BPP	120	425	820
p-TBPP	120	425	1200

Iron foils exposed to *p*-TBPP show a surface layer, which contains more than 40 at. % carbon and 10−20 at. % iron, phosphorus, and oxygen. A second layer,

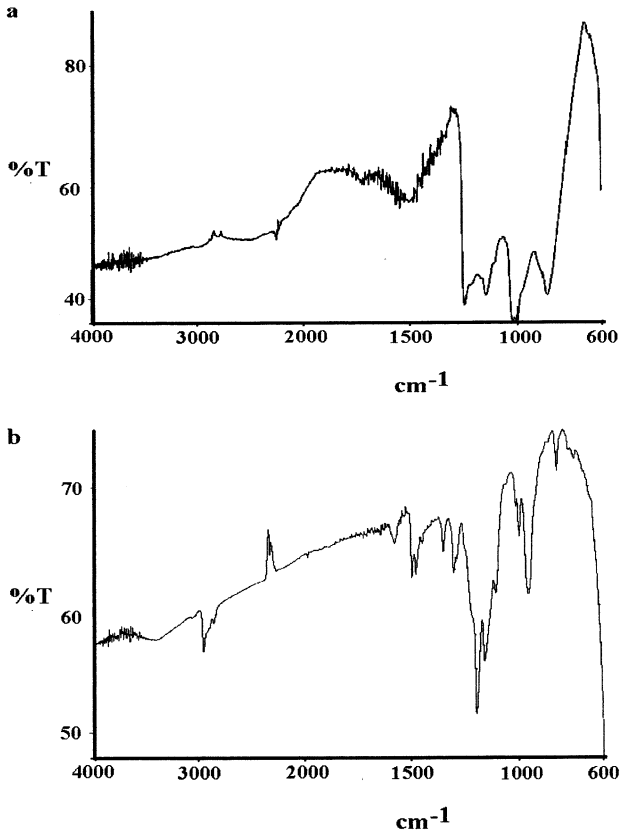

Figure 9. Infrared spectrum of a heavily coated region of a metal coupon exposed to commercial *t*-BPP.

which contains a higher oxygen content and much lower carbon content, forms just below the surface. A third layer, much higher in carbon, appears adjacent to the metal surface. The nature of this layer is not well understood, although iron carbide[26] and amorphous carbon have both been postulated.[21] A comparison of the Auger electron energy with several known compounds[27] indicates that the carbon in the layer is not a pure diamond, graphite, or carbide, suggesting that it is either an amorphous carbon deposit or a mixture of carbon-containing species. The Auger electron energy is intermediate between the energies observed for graphite and diamond.[28]

Differences are observed between samples, which have been exposed to *p*-TBPP as compared with *t*-BPP. The differences are mainly in the level of carbon found in the second layer within the film. The model compounds *p*-TBPP forms a decomposition film with considerably more carbon in the intermediate layer than the commercial mixture. This observation may be in part due to the larger number of aliphatic carbons contained in the model compound.

3. Infrared Spectroscopy. Infrared spectra of the metal coupons were studied to characterize the deposited films further. A typical infrared spectrum is shown in Figure 9. The infrared spectra all share some common features, including absorption bands between 2900 and 3000 cm^{-1}, indicating hydrogen atoms bound to the aromatic rings.[29] A series of bands between 900 and 1100 cm^{-1}, indicating phosphorus−oxygen bonds, were also observed. The intensity of other bands was low, in part due to the very thin films that have been deposited on the metal surface.

The series of bands between 900 and 1100 cm^{-1}, which have been attributed to the P−O bonds within the phosphate ester molecule, are particularly sensitive to details of the phosphate structure.[30] Previous studies have shown that the P−O bands for iron polyphosphate appear at lower energies than P−O bonds for iron phosphate.[31] The infrared spectra observed for the films formed from *t*-BPP and *p*-TBPP have P−O absorptions, which correspond in vibrational energy more closely to those of an iron polyphosphate glass than any of the other forms of iron phosphate. These results are consistent with infrared observations made on bearing surfaces after high-temperature exposure to tricresyl phosphate. Microscopic examination of the metal surface indicates that several different regions exist on the metal surface. These can be characterized as regions that have a thick black coating and those that just appear to be discolored. The infrared spectrum of the discolored regions shows primarily the bands described above, indicating the presence of a bound iron organophosphate. The infrared spectrum of the black coating shows many of the same features with additional bands at 3060 and 1598 cm^{-1}. These features are consistent with the formation of various aromatic compounds, which may be either chemically bound or strongly adsorbed to the metal surface.

Discussion

The results for TCP have provided a qualitative understanding of the thermal degradation of phosphate esters. First, TCP degrades via different pathways, depending on whether the metal surface is present or not. In the absence of metal, the primary degradation product is cresol. In the presence of the metal surface a small amount of cresol is formed, but a number of other products are also formed. TCP is reported to form a lubricious film even at temperatures up to 800 °C in a nitrogen atmosphere and 550 °C in air.[2] The observed difference in reaction products indicates that two different degradation mechanisms exist for TCP. This will be evident in the proposed initial degradation mechanism. There were two major degradation products in all the chromatograms analyzed, cresol and tolyl-TCP. Two paths can explain the formation of cresol. The first path is through the straight thermal degradation of TCP without metal. The proposed thermal degradation mechanisms support theories that the phosphate esters react with a thin iron oxide coating on the surface of the iron foil. In this case, an oxygen atom on the iron surface attacks the phosphorus of the TCP, kicking off a cresol group. Iron-based alloys contain approximately equal numbers of Lewis acid and base sites located on the surface once they have been exposed to atmospheric

(26) Klaus, E. E.; Philips, J.; Lin, S. C.; Wu, N. L.; Duda, J. L. *Tribol. Trans.* **1990**, *33*, 25.
(27) Saba, C. S.; Keller, M. A.; Chao, K. K.; Toth, D. K.; Borchers, M. F.; Waldron, W. M.; Johnson, D. W. Lubricant Performance and Evaluation III. AFRL-PR-WP-TR-1998−2117, 1998; pp 251−253.
(28) Haas, T. W.; Grant, J. T.; Dooley, G. J., III *J. Appl. Phys.* **1972**, *43*, 1853−60.
(29) Silverstein, R. M.; Bassler, G. C.; Morrill, T. C. *Spectrophotometric Identification of Organic Compounds*, 4th ed.; John Wiley and Sons: New York, 1981; pp 95−181.
(30) Molt, K.; Egelkraut, M.; Gottwald, K. H. *Mikrochim. Acta* **1988**, *2*, 63.
(31) Gabelica-Robert, M.; Tarte, P. *J. Mol. Struct.* **1983**, *79*, 251.

oxygen.[32] The attack on the phosphate ester molecule can occur at either acidic or basic sites on the surface. Similar products are observed in the photochemical degradation of triphenyl phosphate.[33] The cresol vaporizes, while what is left stays bonded to the metal. This would help explain the polymeric film formed by TCP: if several molecules of TCP were reacted in this way, multiple phenyl ring systems would be in very close quarters.

The formation mechanism of the tolyl-TCP can also be explained by two mechanisms. The primary mechanism involves the cleavage of a tolyl group at the metal surface. This cleavage forms a stable radical, which attacks another TCP molecule, forming the tolyl-TCP product. However, tolyl-TCP was also formed when no metal was present (in much smaller amounts). This mechanism of tolyl-TCP formation involves a dehydration reaction between cresol and TCP. The cresol formed during the thermal degradation of TCP reacts with TCP, producing the tolyl-TCP and H_2O.

Analysis of the metal surface by Auger shows a multilayered structure. In this structure, partial decomposition of the phosphate ester yields a polyphosphate coating with one bound organic group. Reactions of this type provide for the formation of a complex film containing iron, phosphorus, and oxygen, which does not contain sufficient oxygen to form iron phosphate. It is postulated that the film, being somewhat deficient in oxygen, is actually an iron polyphosphate. The relative lack of oxygen also explains the formation of products where carbon−carbon bonds are formed such as biphenyls and more complex phosphate esters.

Conclusion

The results from TCP and *t*-BPP have provided a qualitative understanding of the metal-catalyzed degradation of phosphate esters. First, the phosphate esters degrade via different pathways. In the absence of metal surface, the primary degradation product is cresol and significant amounts of the phosphate ester remain after 24 h at 450 °C. In the presence of the metal, the products depend on the availability of oxygen at the metal surface. When bound oxygen is plentiful, cresol is the primary product. If there is less oxygen available, additional products such as tolyl-TCP are formed. Once formed, these products further decompose to give lower molecular weight products. In the case of meta isomers of TCP or *t*-BPP, further reaction leads to the formation of fused-ring aromatic compounds.

Acknowledgment. This work was conducted under Contract F33615-93-C-2307 for the United States Air Force, Air Force Research Laboratory, Propulsion Directorate, Wright-Patterson Air Force Base, OH. The Air Force Office of Scientific Research, with Drs. Hugh C. DeLong and Paul C. Trulove as program managers, provided support for this research. Partial support from the Ohio Board of Regents and Dr. Allen Garscaden, Chief Scientist, Propulsion Directorate, WPAFB, is gratefully acknowledged.

CM010921O

(32) Buckley, D. H. Importance and Definition of Materials in Tribology- Status of Understanding. In *New Directions in Lubrication, Materials, Wear and Surface Interactions, Tribology in the 80's*; Loomis, W. R., Ed.; Noyes Publication: Park Ridge, NJ, 1985; pp 18−43.

(33) Okamoto, Y.; Tatsuno, T. *Heteroat. Chem.* **1996**, *7*, 257.